Morphometry of pig coronary venous system

GHASSAN S. KASSAB, DANIEL H. LIN, AND YUAN-CHENG B. FUNG
Center for Biomedical Engineering, University of California, San Diego, La Jolla, California 92093

Kassab, Ghassan S., Daniel H. Lin, and Yuan-Cheng B. Fung. Morphometry of pig coronary venous system. *Am. J. Physiol.* 267 (*Heart Circ. Physiol.* 36): H2100–H2113, 1994.—This is a third part of tripartite morphometric data of the pig coronary blood vessels, giving a complete quantitative description of the arterial tree [Kassab et al., *Am. J. Physiol.* 265 (*Heart Circ. Physiol.* 34): H350–H365, 1993], capillary network [Kassab and Fung, *Am. J. Physiol.* 267 (*Heart Circ. Physiol.* 36): H319–H325, 1994], and venous tree (this article). Together they provide the quantative anatomic foundation for coronary hemodnamics. The coronary venules have a unique morphology. Unlike coronary arterioles, which have cylindrical cross sections and a fairly constant diameter in each segment, the venules have approximately elliptical cross sections, are usually wavy in the longitudinal direction, and often converge like fingers to a hand. Measurements were made with the silicone elastomer casting method on five pig hearts. Data on smaller vessels were obtained from histological specimens by optical sectioning. Data on larger vessels were obtained from vascular casts. Arcading veins and anastomoses on the epicardial surface have a unique topology. Data on the number of vessels in each order, the major and minor axes, length, connectivity matrix, and the fractions of the vessels of a given order connected in series in all orders of vessels of the sinusal and thebesian veins are presented. It is shown that of the blood in the coronary blood vessels of a pig heart 27.4% is in the arteries (>200 μm), 37.1% is in veins (>200 μm), and 35.5% is in microcirculation (<200 μm), of which 89.4% is in the capillaries.

heart; sinusal veins; thebesian veins; venules; arcades; anastomoses; connectivity matrix; diameter-defined Strahler system

THERE IS NO DOUBT that coronary vascular disease is one of the most important problems of the American people and that the current research on coronary blood flow is stagnant. One of the reasons for the lack of progress is that some basic data are missing: for example, a complete quantitative description of the architecture of the coronary blood vessels, the three-dimensional structure of the capillary network in the whole heart, detailed knowledge of the structure, materials, and mechanical properties of the coronary blood vessel wall, and their biological regulation by stress, strain, and time. Atherogenesis is related to stress and strain. Without the basic data named above, however, stress and strain cannot be calculated (neither is there an instrument for in vivo measurement, nor can the nuclear magnetic resonance method meet the challenge). A difficulty in obtaining the desired basic data is the lack of new ideas in theoretical organization of the morphological data on one hand [Horton's idea (12) was published 49 years ago, its improvement by Strahler (29) was published in 1952, and its use by Horsfield in lung was began in 1968] and, on the other hand, a lack of new theories of elasticity and viscoelasticity of the blood vessel, which is composed of nonhomogeneous anisotropic finite strain and nonlinear materials regulated biologically by stress and strain. Any advance would have to break these barriers.

Our objective is to elucidate quantitative morphometric characteristics of the coronary venous system. The importance of this objective is substantiated by epicardial pressure measurements, which have shown that the coronary venous system may account for up to 33% of total coronary resistance during vasodilation (5). A complete set of morphometric data of the coronary venous blood vessels of the pig, which is often considered as a good model for humans (24), is presented on the basis of three new ideas described in the text: the diameter-defined ordering system, the connectivity matrix, and the series-parallel distinction. These data provide a basis to investigate coronary circulation, to predict the pressure-flow relationship, to determine the longitudinal pressure and blood volume distribution, to understand the distribution of coronary blood flow during venous retroperfusion to the ischemic myocardium, and to quantitate vascular remodeling in heart disease.

There are two routes by which coronary venous flow returns to the heart. In one route, blood flows from the great cardiac vein, the posterior vein of the left ventricle, the posterior interventricular vein, the oblique vein of Marshall, and the small cardiac vein into the coronary sinus and anterior cardiac veins on the epicardial surface and empties directly into the right atrium. In another route, blood flows through the smallest cardiac veins of Thebesius to the endocardial surface and drains directly into the heart chambers. Detailed anatomic studies of these coronary veins began in the 19th century and received increased attention in the 20th century, particularly from the clinical point of view regarding the benefits of retroperfusion to the ischemic myocardium (2, 23). For a detailed review of the coronary venous anatomy and circulation, we refer the reader to *The Coronary Sinus* (21). Our data are separated into the categories of sinusal and thebesian veins.

METHODS

Studies were carried out on five farm pigs (Yorkshire and Duroc crosses) weighing 29–31 kg (30.1 ± 0.7 kg) and 3–4 mo of age. The animal and isolated-heart preparations are identical to those described previously (19). Briefly, a KCl-arrested adenosine-dilated heart was perfused with freshly catalyzed silicone elastomer through its major coronary arteries [right coronary artery (RCA), left anterior descending coronary artery (LAD), and left circumflex coronary artery (LCX)]. The arterial perfusion pressure was maintained at 80 mmHg, and the venous outlet pressure was zero (atmospheric) until the elastomer was hardened. The heart was then refrigerated in saline for several days to increase the strength of the silicone elastomer before preparation for histological and cast studies.

For histological studies of the first 4 orders of small venules, a total of 12 plugs of myocardial tissue were removed from each of the right and left ventricles of four pigs. Each plug was

~4 × 4 mm in cross section and extended from epicardium to endocardium. Each plug was mounted on a freezing microtome and serially sectioned, transverse to the radial direction, to thicknesses of 60–80 μm from epicardium to endocardium. Each section was dehydrated with 100% alcohol and cleared with methyl salicylate to render the myocardium transparent and the silicone elastomer-filled microvasculature visible in light microscopy. The arterioles and venules were distinguished on the basis of their topology (19). The topology of the arterioles is treelike, whereas that of venules is rootlike. Morphometry of the venules was done by changing the focal plane through the thickness of the histological section (optical sectioning). An image-processing system described previously (19) was used to measure the dimensions. The venules were viewed with an inverted light microscope (Olympus, optical resolution 0.6 μm at ×600) and displayed on a color video monitor (Sony Trinitron) through a television camera (COHU solid-state camera). The image was grabbed by the computer software and analyzed with a digitizing system.

The widest width of the vessel seen as the cast was rotated around its longitudinal axis was measured between longitudinal tangents to the vessel cast. This width is called the major axis for the purpose of characterizing the vessel size in the determination of order numbers. The narrowest width of the cast, on the other hand, is called the minor axis. If the cross section of the vessel perpendicular to the longitudinal axis was considered as an ellipse, then the major and minor axes characterize the venous cross section.

For the study of the larger veins of *order 4* and up, the elastomer-perfused and -hardened veins were corroded with a 30% KOH solution for several days. After the tissue was washed away, a solid cast of the vasculature was obtained from each heart. The trunks of the arterial and venous trees are easily identified in a cast. The three major coronary arteries were pruned away. The pruning left venous trees with clusters of capillaries. The venous casts were viewed and dissected under a stereo-dissecting microscope (×60, 2.5-μm optical resolution). The cast images were grabbed and analyzed with the digitizing system described above. Each coronary vein was sketched according to the displayed image, and the whole venous tree was reconstructed completely with the segment (vessel between 2 successive points of bifurcation) major axis and segmental length (curvilinear length of longitudinal axis) of each vessel segment measured and recorded.

To measure the minor axis of the lumen of the cast venous vessels, two protocols were used. We either cut a cast vessel transverse to its longitudinal axis and obtained its cross section for measurement or rotated the vessel specimen in the Petri dish on the microscope stage to visualize the minor axis of the vessel. The two methods gave similar results. However, this process was very time consuming; hence we measured only a sample of vessel segments of each order to obtain a mean value of the ratio of the major to minor axis for various orders of vessels.

From the data on major axis of each segment and the sketch of the complete tree, we assigned order numbers to the venous vessels according to the diameter-defined Strahler system described in Ref. 19. For veins, the major axis was used instead of diameter. After ordering the venous system, we combined those segments of the same order but connected in series into elements, counted the number of elements in each order, and obtained their connectivity matrixes. Because some of these were innovations introduced in Ref. 19, a brief explanation is in order.

First, the capillary blood vessels are defined as vessels of *order 0*. The smallest arterioles supplying blood to the capillaries are assigned *order 1*. The smallest venules draining the capillaries are assigned *order −1*. When two arterioles of *order 1* meet, the confluent vessel is *order 2* if its diameter exceeds the diameters of *order 1* vessels by an amount specified by a set of formulas to be given below or remains as *order 1* if the diameter of the confluent is not larger than the amount specified by the formulas. When an *order 2* artery meets another *order 1* artery, the confluent is *order 3* if its diameter is larger by an amount specified by the formulas or remains as *order 2* if its diameter does not increase sufficiently. This process is continued until all arterial segments are arranged in increasing diameter and assigned *orders 1, 2, 3,..., n,....* Similarly, the veins are assigned *orders −1, −2, −3,..., −n,....* A system of using positive integers to identify the order numbers of arteries and negative integers to identify the order number of veins is convenient when we compare the morphology of the veins with that of the arteries.

Now let us explain the diameter-based ordering formulas. A system of assigning order numbers to the branches of a tree was first introduced by Horton (12) and used by him to study the rivulets and rivers in geography. Horton's system was modified by Strahler (29). Horsfield and Gordon (11) and Yen et al. (36) used the Strahler system to study the morphology of the pulmonary veins in humans and cats, respectively. Morphometrists have used the Strahler system in different fields for various applications (3, 6, 7, 9, 10, 25, 26, 31, 34, 35). In our study of the coronary blood vessels of the heart (18, 19), we recognized that the branching pattern of the coronary vascular trees are Strahler in character and that the most important parameter of the branching pattern from the hemodynamic point of view is the diameter of the vessel. The diameters of the branches of any order of a large Strahler tree are stochastic; i.e., they have a mean and a standard deviation (SD). Let the mean and SD of the diameters of arteries of *order n* be denoted by D_n and Δ_n, respectively, and the mean and SD of the major axis of the veins of *order* $-n$ be denoted by D_{-n} and Δ_{-n}, respectively. The real number axis is divided up into intervals marked by the numbers ..., $D_{-n} - \Delta_{-n}$, D_{-n}, $D_{-n} + \Delta_{-n}$, $D_{-n+1} - \Delta_{-n+1}$,..., $D_1 - \Delta_{-1}$, D_{-1}, $D_{-1} + \Delta_{-1}$, $D_1 - \Delta_1$, Δ_1, $D_1 + \Delta_1$,..., $D_n - \Delta_n$, D_n, $D_n + \Delta_n$,.... We now want to redivide the real axis intervals with consecutive order numbers. For this purpose, we define veins of *order* $-n$ to be those veins with diameters in the interval bounded by

$$[(D_{-n-1} + \Delta_{-n-1}) + (D_{-n} - \Delta_{-n})]/2 \qquad (1a)$$

on the left, and

$$[(D_{-n} + \Delta_{-n}) + (D_{-n+1} - \Delta_{n+1})]/2 \qquad (1b)$$

on the right. Similarly, an artery of *order n* is bounded by

$$[(D_{n-1} + \Delta_{n-1}) + (D_n - \Delta_n)]/2 \qquad (1c)$$

on the left, and

$$[(D_n + \Delta_n) + (D_{n+1} - \Delta_{n+1})]/2 \qquad (1d)$$

on the right. We have used *Eqs. 1c* and *1d* in Ref. 19. We shall use *Eqs. 1a* and *1b* in this paper. The virtue and weakness of this approach have been discussed in Ref. 16.

The second innovation introduced in Ref. 19 is to combine all vessel segments of a given order but connected in series into elements. The third innovation of Ref. 19 is to describe asymmetric branching by a connectivity matrix $C(m,n)$, whose element in *row m* and *column n* is the ratio of the total number of elements of *order m*, which spring directly from parent

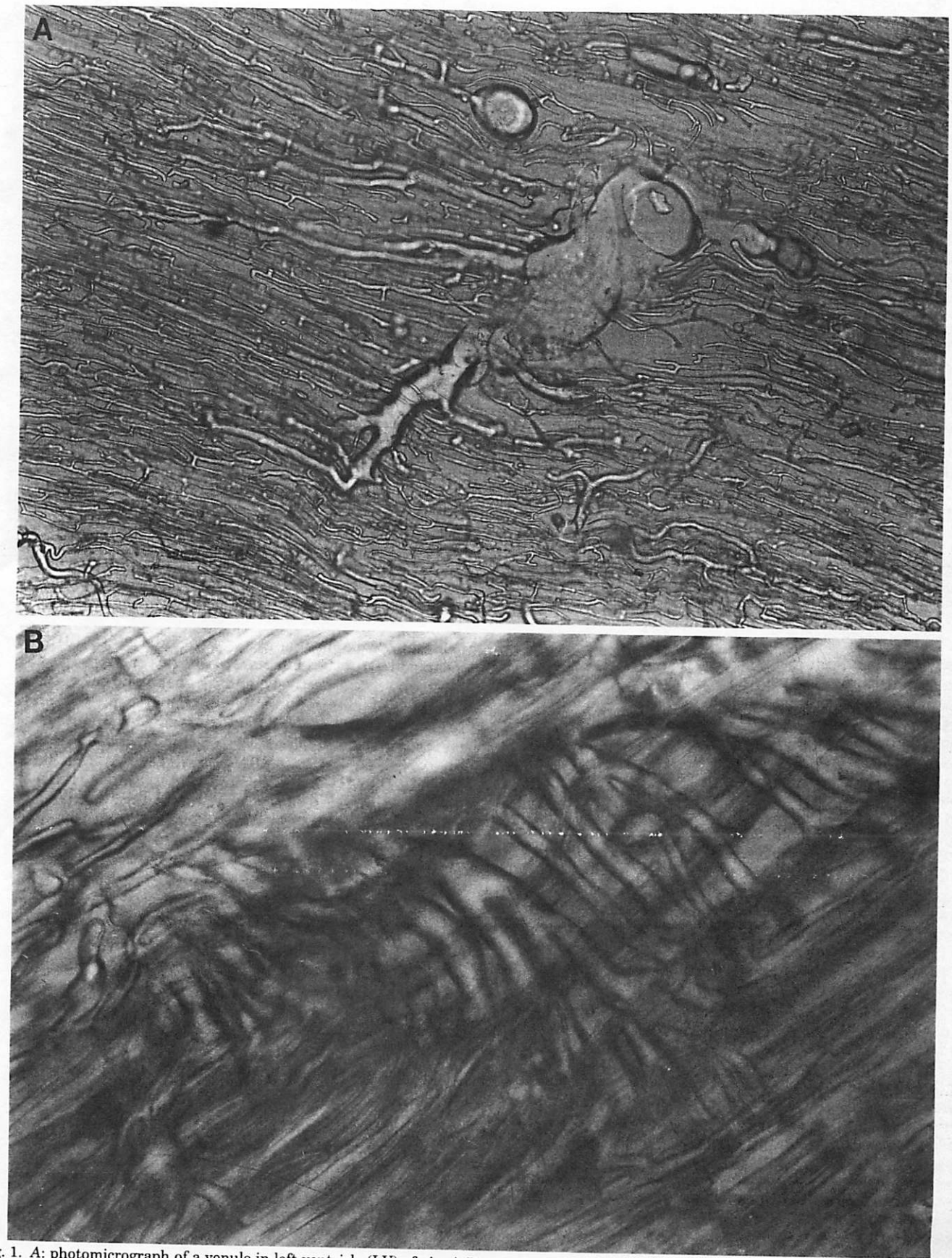

Fig. 1. *A*: photomicrograph of a venule in left ventricle (LV) of pig. A 70-μm-thick section taken at ~1.5 mm from epicardial surface. It shows a large venule draining many capillaries; 1 cm = 71 μm. *B*: photomicrograph of a venule in LV of pig. An 80-μm-thick section taken at ~4.2 mm from epicardial surface. It shows several adjacent venules draining into a small vein; 1 cm = 42 μm.

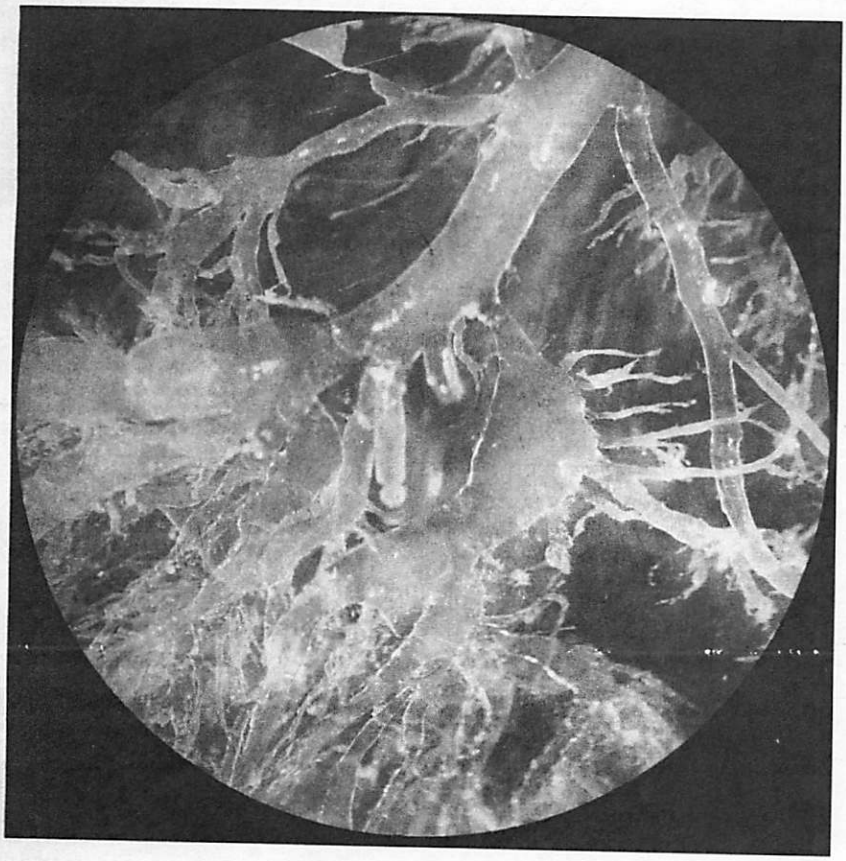

Fig. 2. Cast of coronary sinus veins taken through a stereo-dissecting microscope.

elements of *order n* divided by the total number of elements of *order n*.

RESULTS

The branching pattern of the venules is very different from that of the arterioles. The smallest venules initially lie in the direction of the capillaries they drain, then usually break away from their original directions, and run obliquely toward larger veins. The characteristic branching pattern of endocardial venules has been referred to as the turnip root pattern, ginger root pattern, or as fingers collecting into a hand (see Ref. 1

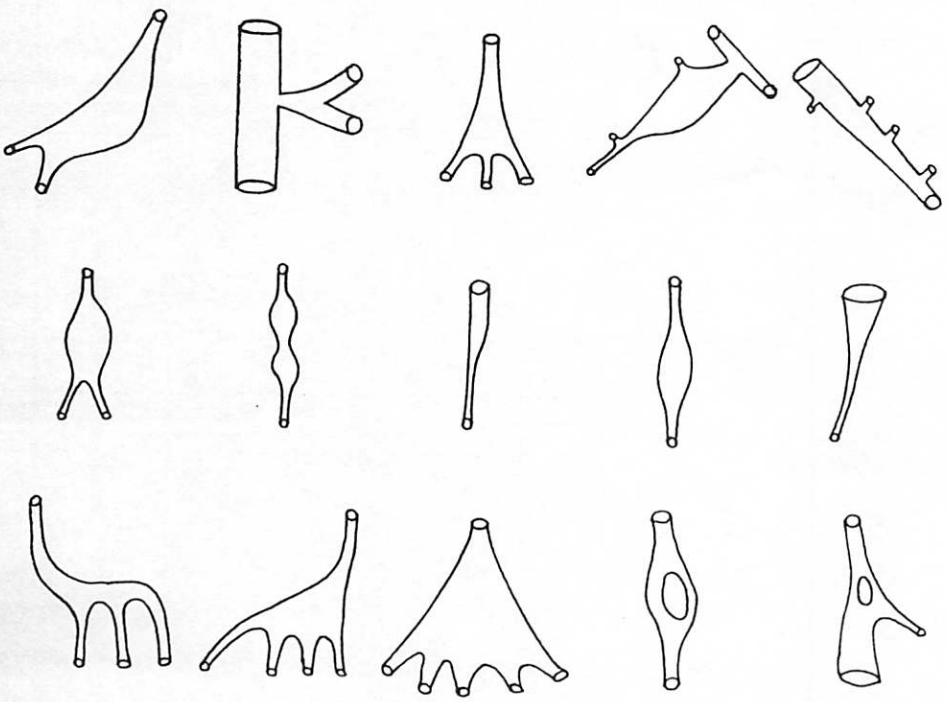

Fig. 3. Schematic reconstruction of some coronary venous patterns.

Table 1. *Major axis, major-to-minor axis ratio, and lengths of vessel segments and elements in each order of vessels in pig coronary sinusal veins*

Order	Segments				Elements				
	D, μm	n	L, mm	n	D, μm	n	L, mm	n	D/minor axis
−1	10.8 ± 1.7	872	0.051 ± 0.041	251	10.6 ± 1.6	121	0.079 ± .054	121	1.32 ± 0.047
−2	17.6 ± 3.0	624	0.056 ± 0.041	313	16.5 ± 2.7	115	0.092 ± .065	115	1.38 ± 0.082
−3	30.0 ± 4.3	425	0.063 ± 0.043	263	29.6 ± 3.2	88	0.117 ± .071	88	1.48 ± 0.100
−4	55.5 ± 13.5	13,719	0.223 ± 0.179	1,948	57.5 ± 11.8	435	0.350 ± .277	435	1.70 ± 0.060
−5	117 ± 25.1	10,238	0.302 ± 0.239	6,408	117 ± 18.7	2,069	0.698 ± .649	2,069	1.83 ± 0.05
−6	206 ± 42.4	6,611	0.367 ± 0.297	6,175	205 ± 25.6	1,713	1.26 ± 1.13	1,711	1.91 ± 0.069
−7	321 ± 63.0	3,572	0.447 ± 0.376	3,435	317 ± 32.7	768	2.08 ± 1.87	768	1.96 ± 0.058
−8	487 ± 97.5	1,785	0.591 ± 0.474	1,705	488 ± 46.5	282	3.62 ± 3.19	282	1.90 ± 0.101
−9	770 ± 154	675	0.857 ± 0.743	662	773 ± 62.4	98	6.07 ± 5.11	98	1.82 ± 0.110
−10	1,192 ± 185	213	1.26 ± 0.967	200	1,165 ± 88.2	39	10.2 ± 8.32	39	1.68 ± 0.148
−11	1,999 ± 731	117	1.72 ± 1.37	106	1,804 ± 464	16	25.8 ± 24.2	14	1.45 ± 0.053
−12	5,919 ± 2,353	24	2.84 ± 1.48	23	5,919	1	71.9	1	1.25 ± 0.145

D, major axis (means ± SD); L, length of segment (means ± SD); n, no. of vessels measured; D/minor axis, major-to-minor axis ratio (means ± SD).

for review). The branching pattern of the endocardial venules is shown in Fig. 1, *A* and *B*. Several adjacent venules can be found draining into a nearby vein as shown in Fig. 1*B*. Figure 2 shows the interesting branching pattern of the venous vessels as seen in a cast. The major axis of the venules has a tendency to fluctuate along the segment unlike arterioles, which have a fairly constant diameter in each vessel segment. Figure 3 shows sketches of several unusual endocardial venous geometries. Trifurcations, quadrifications, and quintifications are more frequent in venules than arterioles. The branching of the whole arterial tree was found to be 98% bifurcations and 2% trifurcations; that of venous trees was found to be 86% bifurcations, 12.8% trifurcations, 1% quadrifications, and 0.2% quintifications. The branching pattern of the endocardial venules is, however, strictly treelike, lacking arcading.

The morphometric data of right and left ventricular (LV) venules, excluding the epicardial venules, were combined, since no statistical differences were found in the venular morphometric data of the two ventricles. Tables 1 and 2 show our experimental results of means ± SD of the major axes, major-to-minor axis ratios, and the length for the segments and elements of sinusal and thebesian veins, respectively. Note that the data of the smallest venules of *orders −1*, *−2*, and *−3* were obtained from histological slides in which it is not possible to distinguish sinusal from thebesian vessels. Hence it is assumed that there is no difference between those two systems at *orders −1*, *−2*, and *−3*; the same data apply to Tables 1 and 2 for these first three orders. In Tables 1 and 2, elements are composed of segments connected in series. Hence in any order the length of elements is larger than the length of segments and the number of elements is smaller than the number of segments. Tables 1 and 2 show that there are a total of 12 orders of veins in the sinusal system, whereas there are only 10 orders of veins in the thebesian system.

Figure 4 shows the relationship between the mean vessel major axis and the order number for the elements of the sinusal and thebesian veins, respectively. Figure 5 shows the relationship between the mean ratio of the major to minor axis and the order number fitted by a fourth-order polynomial. Figure 6 shows the relationship between the mean vessel element length and the order number for the coronary sinusal and thebesian veins, respectively. The curves in Fig. 4 for the sinusal and thebesian veins are fitted by the equations

$$\log_{10} D_n = a + b(n) \qquad (2)$$

where D is the length of the major axis, n is the order

Table 2. *Major axis, major-to-minor axis ratio,and lengths of vessel segments and elements in each order of vessels in pig thebesian veins*

Order	Segments				Elements				
	D, μm	n	L, mm	n	D, μm	n	L, mm	n	D/minor axis
−1	10.8 ± 1.7	872	0.051 ± 0.041	251	10.6 ± 1.6	121	0.079 ± .054	121	1.32 ± 0.047
−2	17.6 ± 3.0	624	0.056 ± 0.041	313	16.5 ± 2.7	115	0.092 ± .065	115	1.38 ± 0.082
−3	30.0 ± 4.3	425	0.063 ± 0.043	263	29.6 ± 3.2	88	0.117 ± .071	88	1.48 ± 0.100
−4	54.4 ± 15.2	4,635	0.235 ± 0.204	1,681	54.8 ± 11.5	492	0.384 ± 0.327	490	1.70 ± 0.060
−5	110 ± 24.0	2,668	0.314 ± 0.228	1,967	111 ± 17.2	718	0.684 ± 0.580	716	1.83 ± 0.052
−6	190 ± 38.8	1,552	0.372 ± 0.323	1,427	189 ± 22.5	399	1.25 ± 1.11	397	1.91 ± 0.069
−7	299 ± 69.7	789	0.443 ± 0.402	760	292 ± 30.6	140	2.44 ± 1.99	138	1.96 ± 0.058
−8	549 ± 116	331	0.682 ± 0.616	318	549 ± 53.5	54	4.21 ± 3.36	62	1.90 ± 0.101
−9	820 ± 135	156	0.812 ± 0.681	154	813 ± 55.6	24	6.23 ± 5.51	24	1.82 ± 0.110
−10	1,171 ± 272	67	0.970 ± 0.587	64	1,184 ± 230	11	9.35 ± 6.67	11	1.68 ± 0.148

Values for D and L are means ± SD and for D/minor axis are means ± SE.

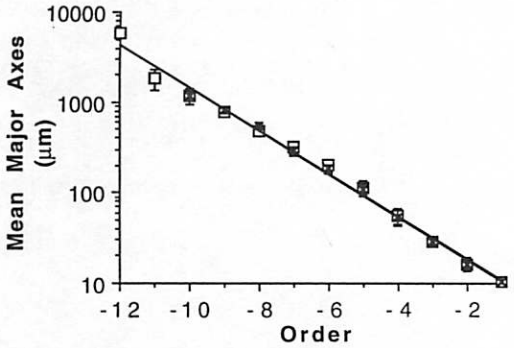

Fig. 4. Relation between average major axis of vessel elements in successive orders of vessels and order number of vessels in sinusal and thebesian veins of pig. Sinusal (□): $a = 0.803$, $b = 0.236$, $R^2 = 0.991$. Thebesian (×): $a = 0.795$, $b = 0.237$, $R^2 = 0.995$.

number, and a and b are two constants. Using the least-squares method, we obtained the empirical constants a and b listed in Fig. 4. *Equation 2* is known as Horton's law (11). The curve in Fig. 4 can be better fitted by adding a trigonometric term (32)

$$\log_{10} D_n = a + b(n) + c \cos [\pi(n)/d] \quad (3)$$

where c and d are additional empirical constants. The physical meaning of the constant b is seen by applying *Eq. 2* first to n then to $n + 1$ and subtracting

$$\log_{10} D_{n+1} - \log_{10} D_n = b \quad (4)$$

Hence

$$D(n+1)/D_n = 10^b \quad (5)$$

Thus 10^b is the ratio of the major axis of the successive generation. The physical meaning of a is obtained by setting n to be -1 in *Eq. 2*

$$a = \log_{10} D_{-1} + b \quad (6)$$

Hence a is the major axis intercept. The physical meaning of c is the amplitude of oscillatory deviation from Horton's law. d is the wavelength of oscillation in terms of order numbers.

The mean element length also obeys Horton's law but with a discontinuity in the slope at *order 3* (see Fig. 6).

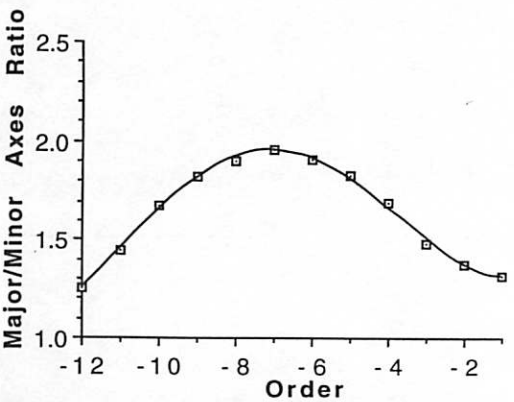

Fig. 5. Relation between average major-to-minor axis ratio of vessels in successive orders of vessels and order number of vessels in coronary veins of pig.

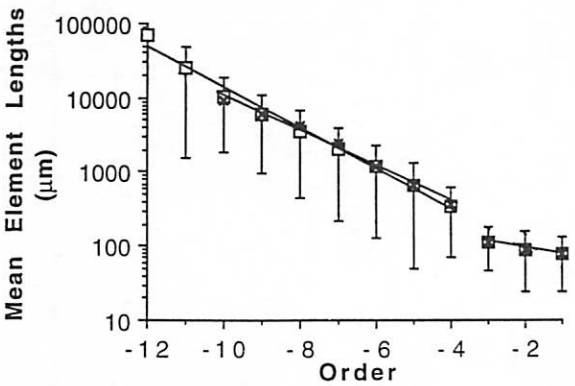

Fig. 6. Relation between average lengths of vessel elements in successive orders of vessels and order number of vessels in sinusal and thebesian veins of pig. Sinusal (□): $a = 1.80$, $b = 0.085$, $R^2 = 0.984$, $n = -1$ to -3; $a = 1.44$, $b = 0.271$, $R^2 = 0.986$, n = greater than -3. Thebesian (×): $a = 1.80$, $b = 0.085$, $R^2 = 0.984$, $n = -1$ to -3; $a = 1.68$, $b = 0.236$, $R^2 = 0.992$, n = greater than -3.

The equation for the element length (L_n) can be written as

$$\log_{10} L_n = a + b(n) \quad (7)$$

with a and b for *orders −1*, *−2*, and *−3* being different from a and b for *orders −4*, *−5*, and above of sinusal and thebesian veins as listed in Fig. 6. Also listed are the correlation coefficients of the fitted curves. It is seen that the correlation is excellent and the element major axis ratios of sinusal and thebesian veins are 1.69 and 1.65, respectively, whereas the element length ratios of sinusal and thebesian veins are 1.77 and 1.61, respectively, for veins of *orders −4*, *−5*, and above but 1.18 and 1.18 for *orders −1*, *−2*, and *−3*.

The "parallel-series" feature of the network of the vessel segments of any given order is characterized by the ratio of the number of segments divided by the number of elements in a given order (designated as S/E). This numbers ratio is presented in Table 3, plotted against the order number n for each system and fitted by a fifth-order polynomial. The fitting is shown in Fig. 7. S/E has the physical meaning of the average number of

Table 3. *Segment-to-element numbers ratio for each order of vessels in sinusal and coronary thebesian veins of pig*

Order	Sinusal Veins		Thebesian Veins	
	S/E	n	S/E	n
−1	1.77 ± 0.90	121	1.77 ± 0.90	121
−2	1.83 ± 1.0	115	1.83 ± 1.0	115
−3	1.91 ± 1.0	88	1.91 ± 1.0	88
−4	1.87 ± 1.2	605	1.88 ± 1.3	518
−5	2.33 ± 1.7	2,382	2.36 ± 1.6	686
−6	3.47 ± 2.7	1,912	3.67 ± 2.8	327
−7	4.71 ± 3.8	786	5.41 ± 3.9	123
−8	6.16 ± 5.0	286	6.05 ± 3.8	42
−9	7.63 ± 5.3	98	7.14 ± 6.1	22
−10	7.66 ± 5.3	38	8.5 ± 4.5	8
−11	10.5 ± 9.0	13		
−12	24	1		

Values are means ± SD. S/E, series-to-element numbers ratio; n, no. of observations.

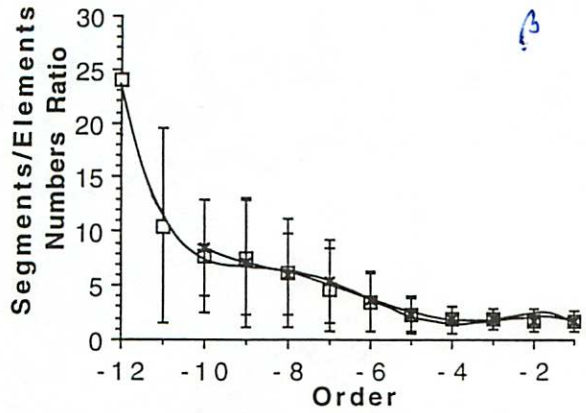

Fig. 7. Relation between average number of segments in series in successive orders of vessels and order number of vessels in sinusal (□) and thebesian (×) veins of pig.

vessel segments in series. It is seen that the largest orders have more segments in series. The connectivity of blood vessels of one order to another is given by the connectivity matrix $[m,n]$. The connectivity matrixes of sinusal and thebesian veins are given in Tables 4 and 5, respectively, which list values as means ± SE.

The total number of elements of each order of the coronary sinusal veins can be computed from information on the number of intact and cut elements and the connectivity matrix by a method given in Ref. 19. When this method was applied to the thebesian veins, we obtain the results, mean values ± propagated errors of the mean, as presented in Table 6. If the total number of venous segments of each order is desired, one need only to multiply the number of elements by the ratio of the number of segments to the number of elements presented in Table 3.

When the number of elements of veins of *order* n, N_n, is plotted against the order number on a semilog paper as in Fig. 8, it is seen that the data can be fitted by a straight line. Thus the regression line is

$$\log_{10} N_n = a - b(n) \qquad (8)$$

The constants a and b obtained by least-squares fitting of data are presented in Fig. 8. The mean ratio of the numbers of vessels of successive orders is called the "branching ratio." The branching ratio is given by the antilog of the absolute value of the slope of the lines of Fig. 8. The element branching ratios of sinusal and thebesian veins are 3.37 and 3.05, respectively.

The data on the major axis, the ratio of the major to minor axis length, and the lengths and number of elements can be used to compute the total cross-sectional area (CSA) and the blood volume in the coronary veins of each order. If the venous cross section is assumed to be elliptical, then A_n is equal to the product of the area of each elliptical element and the total number of elements (see APPENDIX for derivation)

$$A_n = [(\pi/4)D_n^2 N_n]/(\text{major/minor axis})_n \qquad (9)$$

The total blood volume in all elements of a given order,

Table 4. *Connectivity matrix C(m,n) for coronary sinusal veins of pig*

Order	Order											
	−1	*−2*	*−3*	*−4*	*−5*	*−6*	*−7*	*−8*	*−9*	*−10*	*−11*	*−12*
0	2.56 ± 0.073	0.426 ± 0.068	0.347 ± 0.067	0.033 ± 0.008	0.012 ± 0.003	0.020 ± 0.007	0.006 ± 0.003	0	0	0	0	0
−1	0.105 ± 0.028	2.47 ± 0.117	0.773 ± 0.107	0.315 ± 0.023	0.104 ± 0.008	0.103 ± 0.009	0.089 ± 0.014	0.064 ± 0.017	0.066 ± 0.046	0.028 ± 0.028	0	0
−2		0.109 ± 0.031	2.44 ± 0.114	1.01 ± 0.042	0.338 ± 0.015	0.325 ± 0.018	0.303 ± 0.028	0.345 ± 0.063	0.209 ± 0.074	0.083 ± 0.061	0	0
−3			0.067 ± 0.029	2.17 ± 0.040	0.808 ± 0.024	0.649 ± 0.029	0.689 ± 0.050	0.635 ± 0.103	0.505 ± 0.126	0.194 ± 0.118	0.308 ± 0.175	0
−4				0.140 ± 0.015	2.30 ± 0.030	1.97 ± 0.045	2.28 ± 0.102	2.64 ± 0.254	2.64 ± 0.314	1.42 ± 0.332	1.77 ± 0.717	0
−5					0.097 ± 0.007	2.01 ± 0.035	1.81 ± 0.068	2.08 ± 0.139	2.15 ± 0.207	1.64 ± 0.359	2.38 ± 0.712	1
−6						0.168 ± 0.011	1.71 ± 0.045	1.63 ± 0.107	1.60 ± 0.170	0.861 ± 0.150	2.77 ± 0.717	1
−7							0.164 ± 0.016	1.86 ± 0.077	1.85 ± 0.165	1.22 ± 0.219	2.08 ± 0.625	0
−8								0.188 ± 0.029	1.64 ± 0.122	1.33 ± 0.229	2.54 ± 0.938	1
−9									0.231 ± 0.054	1.33 ± 0.149	2.38 ± 0.525	3
−10										0.167 ± 0.063	2.15 ± 0.406	9
−11											0.462 ± 0.268	8
−12												0

Values are means ± SE.

Table 5. *Connectivity matrix C(m,n) for thebesian veins of pig*

Order	Order										
	−1	*−2*	*−3*	*−4*	*−5*	*−6*	*−7*	*−8*	*−9*	*−10*
0	2.56 ± 0.073	0.426 ± 0.068	0.347 ± 0.067	0.067 ± 0.011	0.015 ± 0.005	0.020 ± 0.008	0.014 ± 0.010	0.020 ± 0.020	0	0
−1	0.105 ± 0.028	2.47 ± 0.117	0.773 ± 0.107	0.435 ± 0.029	0.152 ± 0.017	0.130 ± 0.022	0.055 ± 0.019	0.078 ± 0.038	0.042 ± 0.042	0
−2		0.109 ± 0.031	2.44 ± 0.114	0.854 ± 0.029	0.460 ± 0.031	0.311 ± 0.036	0.324 ± 0.062	0.392 ± 0.097	0.458 ± 0.301	0.600 ± 0.400
−3			0.067 ± 0.029	2.03 ± 0.047	0.668 ± 0.034	0.544 ± 0.056	0.641 ± 0.094	0.608 ± 0.163	0.458 ± 0.248	0.600 ± 0.305
−4				0.300 ± 0.022	2.01 ± 0.043	1.76 ± 0.085	2.15 ± 0.197	2.49 ± 0.407	2.25 ± 0.657	2.80 ± 0.533
−5					0.181 ± 0.016	1.84 ± 0.057	1.91 ± 0.158	2.18 ± 0.371	1.83 ± 0.513	2.50 ± 0.401
−6						0.203 ± 0.025	1.90 ± 0.095	1.84 ± 0.268	1.54 ± 0.340	2.20 ± 0.533
−7							0.234 ± 0.040	1.53 ± 0.182	1.37 ± 0.329	1.50 ± 0.428
−8								0.216 ± 0.058	1.37 ± 0.261	1.40 ± 0.221
−9									0.167 ± 0.078	1.90 ± 0.378
−10										0.417 ± 0.193

Values are means ± SE.

Table 6. *Total number of vessel elements in each order of sinusal and coronary thebesian veins of pig*

Order	No. of Vessels	
	Sinusal Veins	Thebesian Veins
−12	1	
−11	16 ± 2	
−10	58 ± 8	10 ± 1
−9	174 ± 30	26 ± 2
−8	541 ± 108	63 ± 4
−7	1,725 ± 380	196 ± 20
−6	4,988 ± 1,200	685 ± 81
−5	16,211 ± 4,104	2,325 ± 340
−4	63,014 ± 16,982	9,713 ± 1,825
−3	167,221 ± 52,204	22,437 ± 5,536
−2	538,990 ± 204,426	61,362 ± 23,154
−1	1,656,943 ± 748,691	167,681 ± 90,148

Values are means ± propagated error.

V_n, is given by

$$V_n = L_n A_n \qquad (10)$$

The results of the total CSA and blood volume calculations are shown in Figs. 9 and 10, respectively. The cumulative volume of whole venous tree is the summation of V_n over n from −1 to −12.

Many arcading venules are found within the epicardial surface of the heart. Figure 11*A* shows an example of an epicardial venous arcade that consists of an interconnection between parts of the same vein. Arcading veins may have multiple feeding vessels but a single draining vessel. Table 7 shows the morphometry of the arcades as a function of the draining vessels. Shown are means ± SD of the arcades diameters and lengths and the number of arcades measured. Epicardial venous arcades were found to have cylindrical cross sections unlike the endocardial venules, which have approximately elliptical cross sections. It can be shown that Horton's law holds for the relationship between the mean arcade diameter and length and the order number of the draining vessel. Horton's law yield a diameter ratio of 1.54 between successive orders of vein and a corresponding length ratio of 1.59. The connectivity of

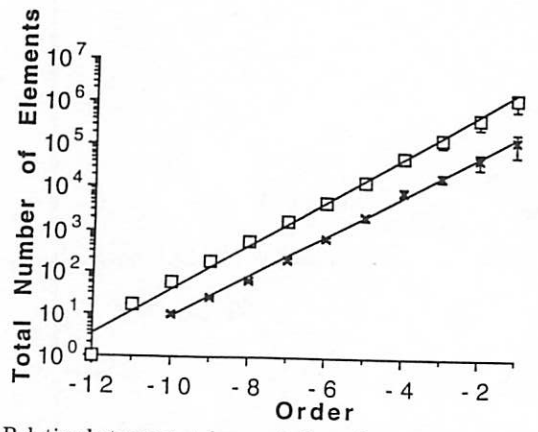

Fig. 8. Relation between total corrected numbers of vessel elements in successive orders of vessels and order number of vessels in sinusal and thebesian veins of pig. Sinusal (□): $a = 6.85$, $b = 0.528$, $R^2 = 0.990$. Thebesian (×): $a = 5.77$, $b = 0.485$, $R^2 = 0.997$.

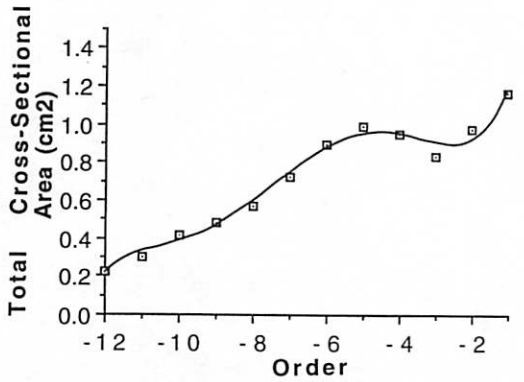

Fig. 9. Relation between calculated total cross-sectional area of coronary venous system in each order and order number of vessels in pig.

the feeding and draining vessels of the arcades can be expressed in terms of a tree/arcade $[m,n]$ connectivity matrix. Table 8 shows the tree/arcade $[m,n]$ connectivity matrix for the venous vessels. The mth row is the order of the vessels draining the arcade, and the nth column is the order of the tree vessels feeding the arcade.

There also exists anastomoses between different veins. Figure 11*B* shows an example of an epicardial anastomoses between two different veins. Venous anastomoses, however, are not restricted to the epicardial surface. They may be endocardial, connecting sinusal to thebesian veins. Anastomotic veins may have multiple feeding vessels but only two draining vessels. Table 9 shows the morphometric data and the connectivity matrix of the anastomoses found as a function of the draining vessels. Means ± SD of the anastomotic vessel diameter and length are shown. Also shown is the tree/anastomoses $[m,n,f]$ connectivity matrix. The anastomoses connect the trunks of two major trees together. There are, however, many trees feeding into the length of the anastomoses. The tree/anastomoses $[m,n,f]$ connectivity matrix shows that for a given orders m and n draining the anastomoses, the order of tree vessels f feeding into the anastomoses.

DISCUSSION

The coronary venous system has a treelike branching pattern except at the epicardial surface, where arcades are found connecting the sinusal veins, and at the endocardial surface, where arcades are found connecting thebesian veins. Tables 1–6 describe the morphometry and connectivity of the treelike sinusal and thebesian veins. It is interesting to compare the morphometric data of the first several orders of veins with those of the arteries (19). The major axes of the first several orders of veins are larger than the diameters of the corresponding arteries, the lengths are shorter, and the numbers are greater. These features imply that the venous system is a lower resistance system. Hence our morphometric data are in agreement with the epicardial micropressure measurements, which have shown that the pressure drop over the first several orders of veins is smaller than that of the corresponding arteries (4, 5, 15, 30).

It is well known that the total coronary CSA and blood volume vary through the cardiac cycle (20). For a maximally vasodilated relaxed myocardium, the total CSA and blood volume of coronary blood vessels of each order are shown in Figs. 9 and 10, respectively, in which the arterial inlet pressure was 80 mmHg and venous outlet pressure was zero (atmospheric). It can be seen that the total CSA of various orders of veins are larger than those of the corresponding orders of arteries (19). The accumulative arterial volume (RCA, LAD, and LCX) is 3.0 ml (19), whereas the accumulative venous volume (sinusal and thebesian trees, arcades, and anastomoses) is 4.1 ml. Our venous volume calculations show that in diastole the thebesian veins contain 5% of the volume of sinusal veins. These values are in agreement with our experimental measurements of the volumes of the venous casts. The cast volume of the entire coronary vasculature was also measured. We found a total coronary vascular volume of 10.4 ml for a 150-g heart (85 g LV). Hence the capillary blood volume is 3.3 ml, obtained by subtracting the arterial and venous volumes from the whole coronary vascular volume. The mass normalized coronary blood volume in the arterial, capillary, and venous compartments is 3.5, 3.8, and 4.9 ml/100 g LV, respectively. The total mass normalized coronary blood volume is therefore 12.2 ml/100 g LV. The mean blood volumes reported for the coronary vasculature range from 4.8 to 14 ml/100 g LV for various species [see critical review by Spaan (28)]. The lower values are underestimates, since those hearts were blotted before determination of blood volume, implying that some of the blood volume from the larger arteries and veins was lost.

The pig heart has arcading veins at the epicardial and endocardial surfaces but no arcading arteries. In other organs (13, 14, 33) arcading veins are accompanied by arcading arteries. The dog heart, for instance, does contain arcading arteries along with arcading veins at the epicardial surface (unpublished observations). The morphometry and connectivity of the pig venous arcades are shown in Tables 7 and 8, respectively. The arcade diameters and lengths are found to obey Horton's law in relation with the order numbers. A system obeying such a law is said to be "fractal." We have shown in *Eqs. 2*, *7*, and *8* and Figs. 4, 6, and 8 that the coronary venous trees of the pig heart have the characteristic of being

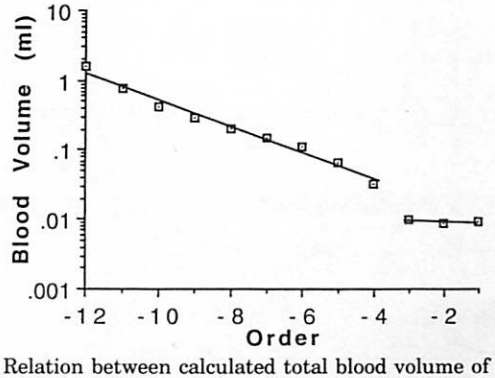

Fig. 10. Relation between calculated total blood volume of coronary venous system in each order and order number of vessels in pig.

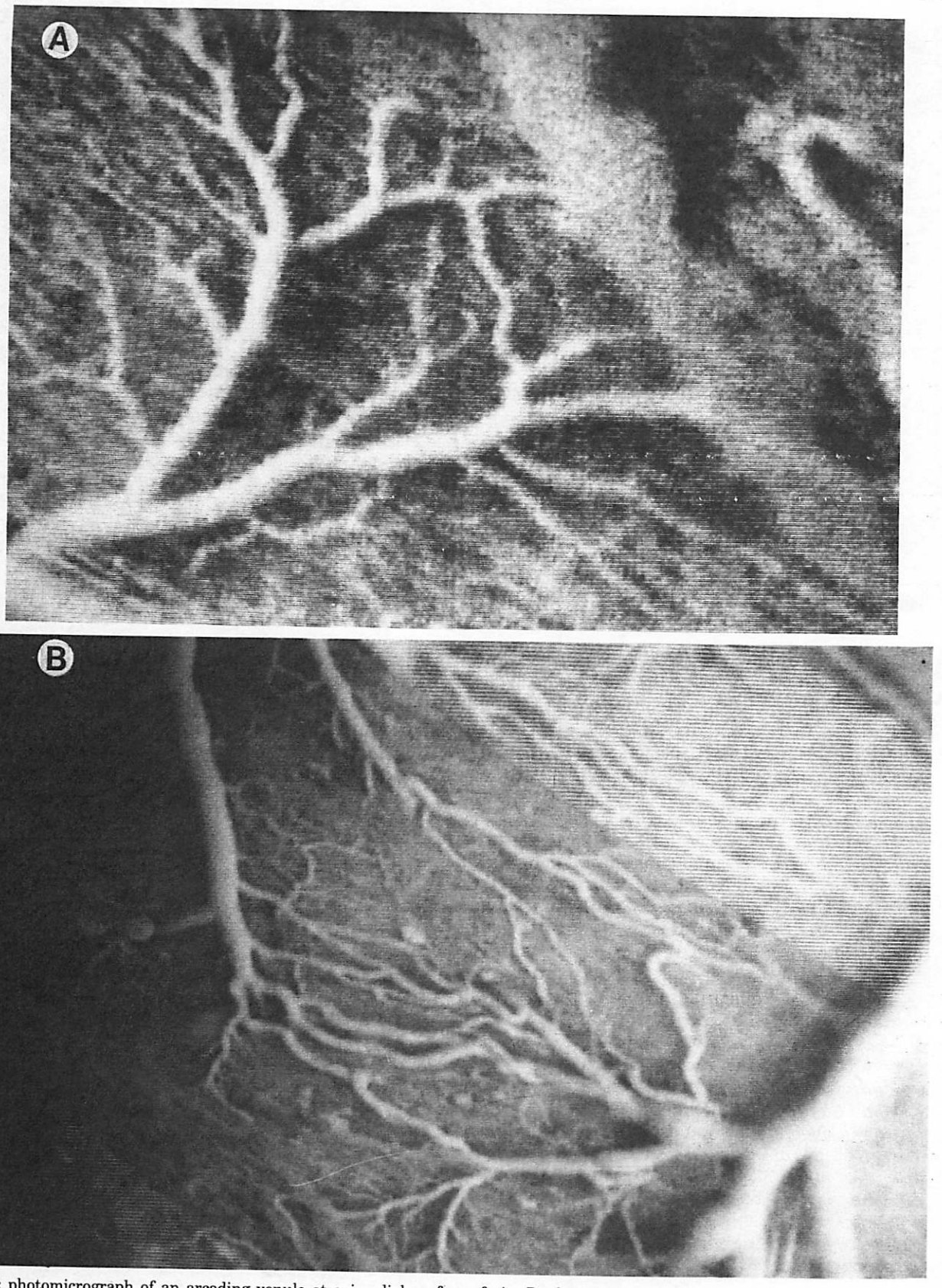

Fig. 11. *A*: photomicrograph of an arcading venule at epicardial surface of pig. *B*: photomicrograph of a venous anastomoses at epicardial surface of pig. These are intravital microscope views of a radiopaque Microfil perfusion of coronary sinusal veins.

Table 7. *Diameters and lengths of venous arcades in each order of draining vessels in pig*

Order	D, μm	L, mm	n
−3	21.2	0.341	1
−4	38.9 ± 13.6	0.568 ± 0.233	11
−5	60.6 ± 18.4	0.645 ± 0.504	18
−6	117 ± 37.1	1.37 ± 1.24	47
−7	180 ± 57.2	2.30 ± 2.08	67
−8	266 ± 86.2	2.95 ± 2.68	29
−9	351 ± 82.1	3.98 ± 3.61	13
−10	460 ± 159	9.02 ± 7.95	10
−11	728	15.5	3

Values are means ± SD. D, diameter of venous arcades; L, length of venous arcades; n, no. of arcades measured.

fractal. In Ref. 19 we have shown that the coronary arteries of the pig are fractal also.

There are other interesting features in the detailed geometry of the coronary veins. Figure 3 shows some features not found in arteries. Some parts of the coronary veins look like a sinus, which is a local dilation of the vessel without branching; other parts look like a sinusoid, which has dense networks of vessels draining into it.

The thebesian and sinusal veins communicate through venous anastomoses, whose morphometric and connectivity data are given in Table 9. These anastomoses are very important when considering the clinical application of retrograde perfusion. Retrograde perfusion through the coronary veins, when the coronary arteries are stenosed, results in less capillary flow than expected due to loss of flow through the thebesian vessels. We have previously demonstrated the relationship between the anatomy of the coronary venous system, myocardial function, and transmural blood flow during coronary venous retroperfusion in pigs (22). Briefly, retrograde perfusion through the coronary sinus or left anterior descending vein drains into the chambers of the heart via anastomoses of the thebesians with the sinusal veins. At low retrograde perfusion pressures, most of the blood is shunted from the capillaries through the lower resistance anastomoses. As the retrograde pressure is increased, the epicardial capillaries begin to fill first while the endocardial flow is still shunted through thebesians. As the retrograde pressure is increased further, transmural filling of the capillaries occurs with eventually all the capillaries throughout the thickness of the heart becoming filled at higher pressures. At those pressures, however, small venules "tear" and microhemorrhage can occur.

Finally, our choice of the characteristic dimension to describe the size of the vessel must be discussed. As mentioned before, the shape of the normal cross section of the coronary vein is neither circular nor elliptical but somewhat irregular. When the plastic cast of a vein is examined while rotating it about its longitudinal axis, one sees that there is one position at which the width is maximum. We call that width the "major axis" of the vessel, as a short hand of the phrase "the length of the major axis of an ellipse that approximate the normal

Table 8. *Tree/arcade connectivity in veins of pig*

Order of Drainers	Order of Feeders										
	−1	−2	−3	−4	−5	−6	−7	−8	−9	−10	−11
−3	2	1	1								
−4	0.222 ± 0.147	0.667 ± 0.441	0.778 ± 0.324	0.889 ± 0.201							
−5	0.210 ± 0.164	0.316 ± 0.265	0.526 ± 0.280	0.842 ± 0.245	0.737 ± 0.129						
−6	0.120 ± 0.084	0.200 ± 0.070	0.320 ± 0.097	1.08 ± 0.216	0.780 ± 0.112	0.820 ± 0.089					
−7	0.061 ± 0.030	0.308 ± 0.082	0.646 ± 0.157	1.60 ± 0.290	0.908 ± 0.158	0.661 ± 0.103	0.969 ± 0.069				
−8	0.156 ± 0.065	0.625 ± 0.257	0.812 ± 0.275	1.97 ± 0.470	1.25 ± 0.246	0.719 ± 0.157	0.594 ± 0.134	0.812 ± 0.070			
−9	0.385 ± 0.311	0.385 ± 0.266	0.692 ± 0.286	1.54 ± 0.704	1.23 ± 0.361	1.00 ± 0.438	1.00 ± 0.320	0.692 ± 0.208	0.846 ± 0.191		
−10		0.250 ± 0.250	0.375 ± 0.375	2.62 ± 0.905	1.50 ± 0.627	1.00 ± 0.500	0.750 ± 0.250	1.25 ± 0.453	0.500 ± 0.267	0.750 ± 0.164	
−11		0	0.333 ± 0.333	1.67 ± 0.882	3.00 ± 2.00	3.67 ± 2.18	0.667 ± 0.333	1.67 ± 0.882	1.33 ± 0.882	1.00 ± 0.577	0.667 ± 0.333

Table 9. *Morphometry and connectivity of tree/anastomoses in veins of pig*

Order of Drainers	D, μm	L, mm	Order of Feeders											
			−1	*−2*	*−3*	*−4*	*−5*	*−6*	*−7*	*−8*	*−9*	*−10*	*−11*	*−12*
−6, −6	120	2.04	0	1	1	5	1.5	2.5	0	0	0	0	0	0
−7, −8	234	4.94	0	1	2	4	2.5	1.5	0.5	0	0	0	0	0
−7,−10	249	3.35	0	0	0	0	0	1	1	1	0	1	0	0
−8, −8	274	5.90	0	1	2	7	8	3	0	0	0	0	0	0
−8,−10	228	4.34	1	1	0	5	5	1	2	1	0	1	0	0
−11,−12	655	26.4	0	0	3	15	16	5	7	6	0	1	0	1
−12,−12	741	41.6	0	0	0.5	6	10	5.5	4.5	2.5	2	2	1	2

Values are means. *D*, anastomoses diameter; *L*, anastomoses length.

cross section of a vessel by a plane perpendicular to the longitudinal axis."

From the point of view of hemodynamics, it can be argued that if one approximates the venous cross section as an ellipse, then the length of the minor axis is important. We have acknowledged this and presented data on the ratio of the major to minor axis (Table 1) but noted that the measurement of the minor axis was time consuming. Other important parameters of the normal section are the CSA, the length of the circumference, the resistance to Poiseuillian flow, or the coefficient of the ratio of flow divided by pressure gradient. These parameters are related to the lengths of the major and minor axes as given in APPENDIX.

The morphometric data on the coronary venous system, along with that of the coronary arterial trees (19) and capillary network (17), completes our statistical description of the coronary vascular circuit in diastole. Hemodynamic analysis can now be done for a specific circuit or for a selected set of special circuits, all of which are consistent with the morphometric data measured.

APPENDIX

Relationship Between Geometric and Hemodynamic Parameters of an Elliptical Tube and Lengths of Its Major and Minor Axes

If the normal cross section of a vein is approximated by an ellipse, then, relative to a set of rectangular Cartesian coordinates x and y with origin located at the center, the parametric equations of the ellipse with a semimajor axis a and a semiminor axis b are

$$x = a \cos \theta; \qquad y = b \sin \theta \tag{11}$$

The CSA is

$$\begin{aligned} \text{area} &= 1/2 \oint (x\mathrm{d}y + y\mathrm{d}x) \\ &= 1/2 \int_0^{2\pi} (ab \cos^2\theta + ab \sin^2\theta)\mathrm{d}\theta \\ &= \pi ab \end{aligned} \tag{12}$$

An equivalent circle of radius R_e will have the same area if

$$\pi R_e^2 = \pi ab \tag{13a}$$

or

$$R_e = (ab)^{1/2} = a(b/a)^{1/2} \tag{13b}$$

Table 1 shows that (a/b) varies from 1.25 to 1.96 for vessels between *orders −1* and *−12*. Hence R_e varies between $0.714a$ and $0.895a$.

The circumferential length of the ellipse is

$$\begin{aligned} \text{circumference} &= \oint (\mathrm{d}x^2 + \mathrm{d}y^2)^{1/2} \\ &= \int_0 2\pi (a^2 \sin^2\theta + b^2 \cos^2\theta)_{1/2}\, \mathrm{d}\theta \end{aligned} \tag{14}$$

which is an elliptical integral involving a and b. It may be argued that the cross-sectional shape of a vein is sensitive to internal pressure, especially if the transmural pressure is negative, when the compression of the wall causes elastic instability and buckling, whereas the circumferential length remains constant in the buckling process. Hence the circumferential length is a more stable parameter than the major and minor axes a and b. It is, however, difficult to measure this length, and its value depends on the smoothness of the wall and any irregularity. We do not think that it is practical to measure the circumferential length of the normal section of the coronary veins.

The parameters relevant to the flow can be derived from the Navier-Stokes equation. For a steady longitudinal flow of a Newtonian viscous fluid in a long cylindrical tube of elliptical cross section subjected to a constant pressure gradient. In analogy to the exact solution of flow in a circular cylinder, the velocity profile (u)

$$u = 2\,U[1 - (x/a)^2 - (y/b)^2] \tag{15}$$

satisfies the Navier-Stokes equation and the boundary condition that u is zero on the elliptical wall described by *Eq. 11*. U is the mean velocity over this section. With *Eq. 15*, the Navier-Stokes equation yields

$$\mathrm{d}P/\mathrm{d}x = -\,4\mu U[a^2 + b^2)/(a^2\, b^2)] \tag{16}$$

where μ is the coefficient of viscosity of the fluid, x is the length along the longitudinal axis of the tube, and $\mathrm{d}P/\mathrm{d}x$ is the pressure gradient. Then the volume rate of flow (Q) is

$$Q = \text{area}\, U = \pi ab\, U = -\,\pi/4\mu[(a^3 b^3)/(a^2 + b^2)]\mathrm{d}P/\mathrm{d}x \tag{17}$$

The conductance is given by the coefficient

$$\text{conductance} = \pi/4\mu L[(a^3\, b^3)/(a^2 + b^2)] \tag{18}$$

where L is the length of the tube. The resistance to flow is given by the inverse of conductance

$$\text{resistance} = 4\mu L/\pi[(a^2 + b^2)/(a^3\, b^3)] \tag{19}$$

Equations 15–19 show that a and the ratio b/a are the most important parameters of venous blood flow in which the Womersley number is < 1.

Finally, if the cross section is very narrow, the normal cross section may be better approximated as a rectangular slit rather than an ellipse. If h represents the thickness of the slit and the tube is rigid, the dP/dx is related to the mean flow velocity by the equation

$$dP/dx = -\mu U h^{-2} F \qquad (20)$$

in which F is a number that depends on the structure of the slit, red cell dimensions, and hematocrit. In this case the elasticity of the tube becomes very important to hemodynamics. Details of this type of analysis is given by Fung (Ref. 8, p. 310–332). In the present paper we found the pig coronary veins not to be very narrow; a/b lies in the range of 1.25–1.96 (see Table 1). However, it is conceivable that the cross section of the coronary veins may become very narrow at certain places in systolic condition due to contraction of the heart, muscle force, and ventricular pressure. At the sluicing gates of the "waterfall phenomenon" in coronary blood flow, the cross section is believed to be very narrow. The waterfall theory is discussed at length by Spaan (27).

In summary, we can say that the length of semimajor axis a is significant in hemodynamics. The length of the semiminor axis b is also important, but not necessarily much more so except in buckled veins as in waterfall phenomenon. Hence in this article we present the morphometric data of a and the ratio a/b. To base the order numbering system on a, however, is because a is easier to measure than b, and the data on a are more accurate.

We thank Vincent Dickow, Meena Joshi, Karin Obergfell, Tina Patela, and Morris Yen for excellent technical expertise and effort in collecting data on the venous vessels.

This research is supported by National Heart, Lung, and Blood Institute Training Grants HL-07089 and HL-43026, the American Heart Association, California Affiliate, through Postdoctoral Fellowship 90–51 (to G. S. Kassab), and National Science Foundation Grant BCS-89–17576.

Address for reprint requests: G. S. Kassab, Center for Biomedical Engineering, University of California, San Diego, 9500 Gilman Dr., La Jolla, CA 92093–0412.

Received 5 November 1993; accepted in final form 10 May 1994.

REFERENCES

1. **Anderson, W. D., B. G. Anderson, and R. J. Seguin.** Microvasculature of the bear heart demonstrated by scanning electron microscopy. *Acta Anat.* 131: 305–313, 1988.
2. **Beck, C. S., E. Stanton, W. Batiuckok, and E. Leiter.** Revascularization of heart by graft of systemic artery into coronary sinus. *J. Am. Med. Assoc.* 137: 436–442, 1948.
3. **Berry, M., E. M. Anderson, T. Hollingworth, and R. M. Flinn.** Computer technique for the estimation of the absolute three dimensional array of basal dendritic fields using data from projected histological sections. In: *Stereology 3*. Oxford, UK: Blackwell Scientific, 1972.
4. **Chilian, W. M., C. L. Eastham, and M. L. Marcus.** Microvascular distribution of coronary vascular resistance in beating left ventricle. *Am. J. Physiol.* 251 (*Heart Circ. Physiol.*20): H779–H788, 1986.
5. **Chilian, W. M., S. M. Layne, E. C. Klausner, C. L. Eastham, and M. L. Marcus.** Redistribution of coronary microvascular resistance produced by dipyridamole. *Am. J. Physiol.* 256 (*Heart Circ. Physiol.* 25): H383–H390, 1989.
6. **Cumming, G., R. Henderson, K. Horsfield, and S. S. Singhal.** The functional morphology of the pulmonary circulation. In: *The Pulmonary Circulation and Interstitial Space*, edited by A. P. Fishman and H. H. Hecht. Chicago, IL: Univ. of Chicago Press, 1969, p. 327–338.
7. **Fenton, B. M.** *Topographical Stimulation of the Blood Vessels of the Human Bulbar Conjunctiva and Application to Pressure-Flow Relationships* (PhD thesis). La Jolla: Univ. of California, San Diego, 1980.
8. **Fung, Y. C.** *Biodynamics: Circulation.* New York: Springer-Verlag, 1984.
9. **Horsfield, K.** Pulmonary airways and blood vessels considered as confluent trees. In: *The Lung: Scientific Foundations*, edited by R. G. Crystal, J. B. West, P. J. Barnes, N. S. Cherniak, and E. R. Weibel. New York: Raven, 1991, p. 721–727.
10. **Horsfield, K., and G. Cumming.** Morphology of the bronchial tree in man. *J. Appl. Physiol.* 24: 373–383, 1968.
11. **Horsfield, K., and W. I. Gordon.** Morphometry of pulmonary veins in man. *Lung* 159: 211–218, 1981.
12. **Horton, R. E.** Erosional development of streams and their drainage basins; hydrophysical approach to quantitative morphology. *Bull. Geol. Soc. Am.* 56: 275–370, 1945.
13. **Johnson, P. C.** *Peripheral Circulation.* New York: Wiley, 1978.
14. **Kaley, G., and B. M. Altura.** *Microcirculation.* Baltimore, MD: University Park, 1977, vol. 1 and 2.
15. **Kanatsuka, H., K. G. Lamping, C. L. Eastham, M. L. Marcus, and K. C. Dellsperger.** Coronary microvascular resistance in hypertensive cats. *Circ. Res.* 68: 726–733, 1991.
16. **Kassab, G. S.** *Morphometry of the Coronary Arteries in the Pig* (PhD thesis). La Jolla: Univ. of California, San Diego, 1990.
17. **Kassab, G. S., and Y.-C. Fung.** Topology and dimensions of pig coronary capillary network. *Am. J. Physiol.* 267 (*Heart Circ. Physiol.* 36): H319–H325, 1994.
18. **Kassab, G. S., K. Imoto, F. C. White, C. A. Rider, Y.-C. Fung, and C. M. Bloor.** Coronary arterial tree remodeling in right ventricular hypertrophy. *Am. J. Physiol.* 265 (*Heart Circ. Physiol.* 34): H366–H375, 1993.
19. **Kassab, G. S., C. A. Rider, N. J. Tang, and Y.-C. Fung.** Morphometry of pig coronary arterial trees. *Am. J. Physiol.* 265 (*Heart Circ. Physiol.* 34): H350–H365, 1993.
20. **Levy, B. I., J. L. Samuel, A. Tedgui, V. Kotelianski, F. Marottee, P. Poitevin, and R. S. Chadwick.** Intramyocardial blood volume measurement in the left ventricle of rat arrested hearts. In: *Cardiovascular Dynamics and Flow*, edited by P. Brun, R. S. Chadwick, and B. I. Levy. Paris: INSERM 1988, p. 65–71.
21. **Mohl, W., E. Wolner, and D. Glogar** (Editors). *The Coronary Sinus. Proceedings of the 1st International Symposium on Myocardial Protection via the Coronary Sinus.* New York: Springer-Verlag, 1984.
22. **Oh, B.-H., M. Volpini, M. Kambayashi, K. Murata, H. A. Rockman, G. S. Kassab, and J. Ross.** Myocardial function and transmural blood flow during coronary venous retroperfusion in pigs. *Circulation*: 1265–1279, 1992.
23. **Prinzmetal, M., B. Simkin, H. C. Bergman, and H. E. Kruger.** Studies on the coronary circulation. II. *Am. Heart J.* 33: 420–442, 1947.
24. **Sarjant, S., F. C. White, and C. M. Bloor.** Myocardial morphometric characteristics in swine. *Circ. Res.* 49: 434–441, 1981.
25. **Singhal, S., R. Henderson, K. Horsfield, K. Harding, and G. Cumming.** Morphometry of the human pulmonary arterial tree. *Circ. Res.* 23: 190–197, 1973.
26. **Skalak, T. C., G. W. Schmid-Schoenbein, and B. W. Zweifach.** Topological and morphological studies of the microvascular network in rat spinotrapezius muscle. *Int. J. Microcirc.* 1: 321–322, 1982.
27. **Spaan, J. A. E.** *Coronary Blood Flow: Mechanics, Distribution, and Control.* Boston, MA: Kluwer Academic, 1991.
28. **Spaan, J. A. E.** Coronary diastolic pressure-flow relation and zero flow pressure explained on the basis of intramyocardial compliance. *Circ. Res.* 56: 293–309, 1985.
29. **Strahler, A. N.** Hypsometric (area altitude) analysis of erosional topology. *Bull. Geol. Soc. Am.* 63: 1117–1142, 1952.
30. **Tillmanns, H., M. Steinhausen, H. Leinberger, H. Thederan, and W. Kubler.** Pressure measurements in the terminal vascular bed of the epimyocardium of rats and cats. *Circ. Res.* 49: 1202–1211, 1981.

31. **Ting, A. C.** *Topology of the Vascular Tree and Elasticity of the Arterioles in the Retina of the Rat* (PhD thesis). La Jolla: Univ. of California, San Diego, 1983.
32. **West, B. J., V. Bhargava, and A. L. Goldberger.** Beyond the principle of similitude: renormalization in the bronchial tree. *J. Appl. Physiol.* 60: 1089–1097, 1986.
33. **Wideman, M. P., R. F. Tuma, and H. N. Mayrovitz.** *An Introduction to Microcirculation.* New York: Academic, 1981.
34. **Woldenberg, M. J.** Hierarchial systems: cities, rivers, alpine glaciers, bovine livers, and trees. In: *Geography and Properties of Surfaces Series.* Cambridge, MA: Harvard Univ. Press, 1968.
35. **Yen, R. T., F. Y. Zhuang, Y. C. Fung, H. H. Ho, H. Tremer, and S. S. Sobin.** Morphometry of cat's pulmonary venous tree. *J. Biomech. Eng.* 106: 131–136, 1984.
36. **Yen, R. T., F. Y. Zhuang, Y. C. Fung, H. H. Ho, H. Tremer, and S. S. Sobin.** Morphometry of the cat's pulmonary venous tree. *J. Appl. Physiol.* 55: 236–242, 1983.